

**Paper for the Special Session on Nanostructured Materials at the
50th AIAA/ASME/ASCE/AHS/ASC
Structures, Structural Dynamics and Materials Conference and Exhibit**

A Continuum-Atomistic Analysis of Transgranular Crack Propagation in Aluminum

V. Yamakov^{*}, E. Saether[†], and E. Glaessgen[‡]

NASA Langley Research Center, Hampton, VA, 23681

Abstract

A concurrent multiscale modeling methodology that embeds a molecular dynamics (MD) region within a finite element (FEM) domain is used to study plastic processes at a crack tip in a single crystal of aluminum. The case of mode I loading is studied. A transition from deformation twinning to full dislocation emission from the crack tip is found when the crack plane is rotated around the $[11\bar{1}]$ crystallographic axis. When the crack plane normal coincides with the $[112]$ twinning direction, the crack propagates through a twinning mechanism. When the crack plane normal coincides with the $[011]$ slip direction, the crack propagates through the emission of full dislocations. In intermediate orientations, a transition from full dislocation emission to twinning is found to occur with an increase in the stress intensity at the crack tip. This finding confirms the suggestion that the very high strain rates, inherently present in MD simulations, which produce higher stress intensities at the crack tip, over-predict the tendency for deformation twinning compared to experiments. The present study, therefore, aims to develop a more realistic and accurate predictive modeling of fracture processes.

^{*} National Institute of Aerospace.

[†] Durability, Damage Tolerance, and Reliability Branch, MS/188E, AIAA Member.

[‡] Durability, Damage Tolerance, and Reliability Branch, MS/188E, AIAA Associate Fellow.

I. Introduction

Physics-based modeling of fracture begins at the nanometer-scale where atomistic simulation is used to predict the formation, propagation, and interaction of fundamental damage mechanisms. These mechanisms include dislocation formation and interaction, interstitial void formation, and atomic diffusion. The development of these damage mechanisms progress into microscale processes such as local plasticity and small crack formation. Ultimately, damage progression leads to macroscopic failure modes such as plastic yielding of components and large cracks exhibiting Mode I, II, and III deformation.

Fracture inherently involves mechanisms that operate at a broad range of time and length scales – atomistic bond breaking at the crack tip, dislocation-governed plasticity in the damage zone near the crack tip, and statistically homogenized elasto-plastic properties of the material that influence the crack behavior at larger length scales. Multiscale modeling strategies have been developed to study these fundamental mechanisms while keeping the problem computationally tractable. Multiscale analyses attempt to bridge length scales by providing different physics-based models that can most appropriately represent damage mechanisms at each scale. These methods are especially useful in modeling of fracture in ductile metals, such as aluminum, which is the focus of this study.

Recently, a number of atomistic simulation studies¹⁻⁵ on crack propagation in aluminum have been published. The results of these investigations show that two main mechanisms of crack propagation operate. These mechanisms are propagation through deformation twinning, and propagation through the emission of full dislocations from the crack tip. However, some of these results disagree with experiment². The experimentally observed dominant deformation mode is dislocation slip, while deformation twinning is rarely found. Whereas, the simulations significantly and systematically overestimate the degree of twinning in pure aluminum. This discrepancy between simulations and experiments has attracted considerable attention among researchers^{3,5} because it prevents the reliable and accurate modeling of fracture in particular, and puts doubt on the reliability of the atomistic simulations in general. Most likely, the source of this discrepancy is related to the very different length (nanometers vs millimeters) and time

(nanoseconds vs seconds) scales at which simulations and experiments are usually performed. Nonetheless, the exact mechanism of how these length and time scales affect the propagation process remains unclear.

In an attempt to resolve the issue, Tadmor and Hai³ systematically studied the role of crystallographic orientation of the crack plane on the propagation mechanism. Their assumption was that the constraint imposed by the boundary conditions (dimensionality constraints in a periodic system or surface effects in very thin specimens)³ used for systems of very small sizes in atomistic simulations inhibit dislocation slip and favor twinning.

More recently, Warner et al.⁵ suggested that the crack propagation mechanism is strongly affected by the rate of propagation through the required applied stress intensity at the crack tip. To obtain a measurable propagation in the time frame of the simulation (a few nanoseconds), much larger stress intensities have to be applied as compared to the experimental time frame (seconds). According to Warner et al.⁵, higher stress intensities favor twinning, and thus twinning is more often found in simulations than in experiments.

The present study investigates in detail the conditions responsible for twinning or dislocation emission from a crack tip under Mode I loading. A recently developed embedded statistical coupling method (ESCM)^{6,7} for concurrent multiscale modeling is used. The approach is based on the construction of a coupled atomistic-continuum model. In this method, an atomistic domain is embedded within a larger continuum domain (Fig. 1). The circular atomistic region containing the crack tip is simulated using molecular dynamics (MD), while the surrounding continuum region is simulated using the finite element (FE) method. The authors have previously used the ESCM approach to study intergranular fracture along a grain boundary in aluminum⁸. The same approach is applied here to study transgranular fracture in a single crystal of aluminum.

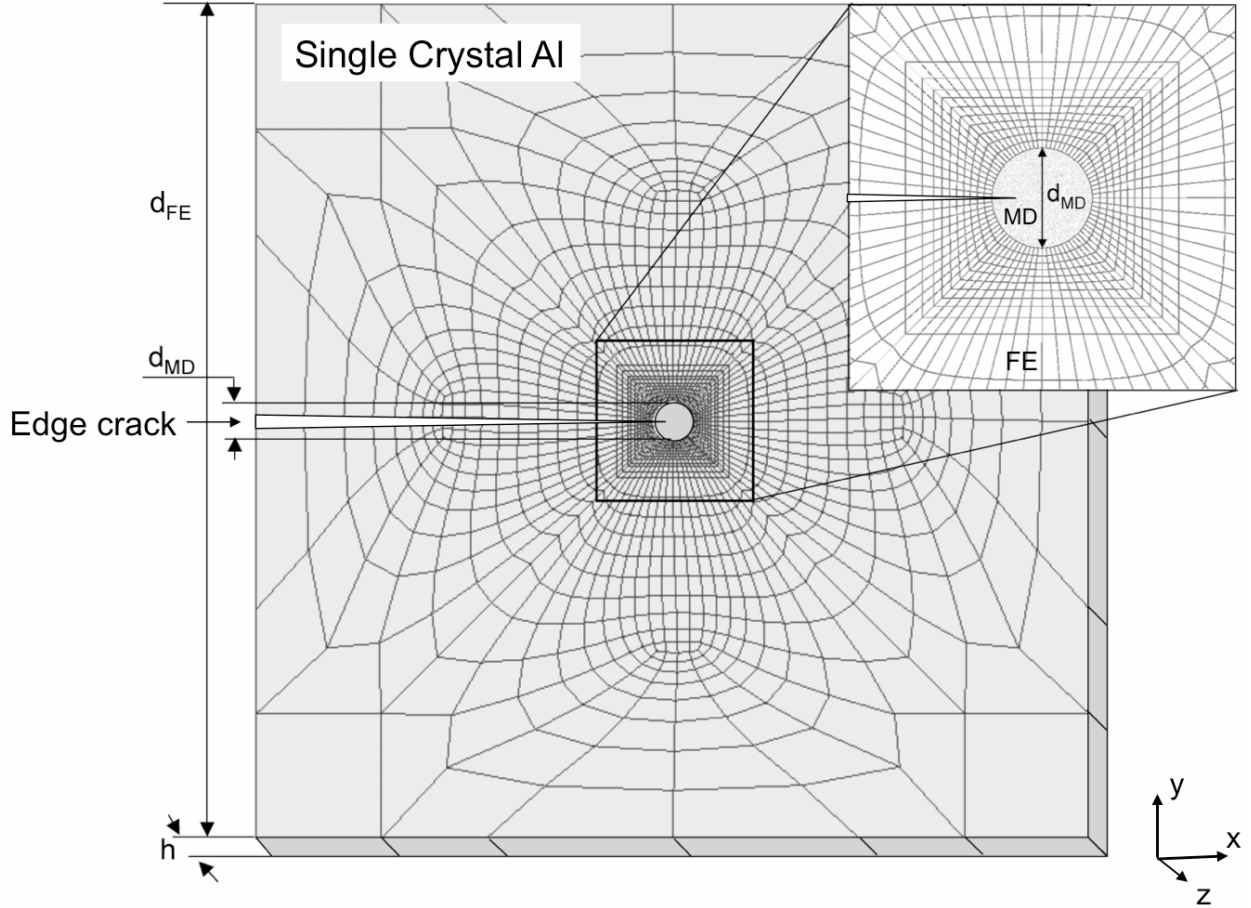


Figure 1: Model geometry of the MD-FEM coupled system with an embedded edge crack ending inside the MD domain.

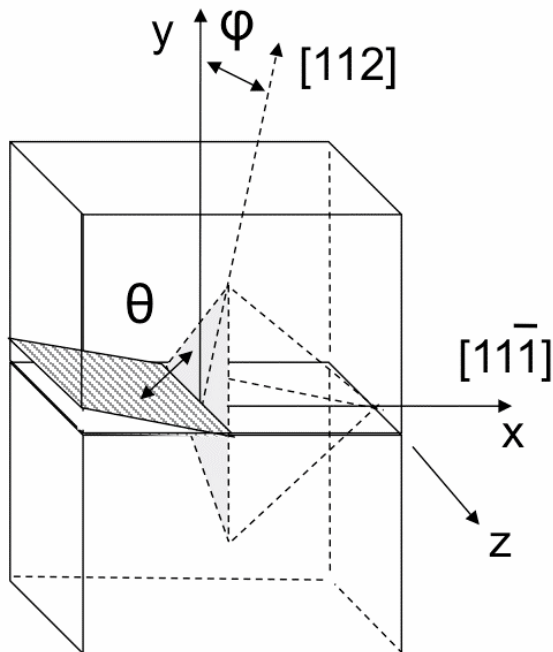
II. The Simulation Approach

The simulation approach used in this study, based on the ESCM, is a coupled atomistic-continuum model that allows a large atomistic domain (containing 10^5 or more atoms) to be embedded within a continuum domain of micron dimensions. The atomistic domain is simulated using MD, where the interatomic forces are represented by an atomistic potential suitably fitted to reproduce the material properties of aluminum⁹. The continuum domain is simulated by using the FEM with anisotropic elastic properties derived from the aluminum potential at room temperature (300K). The ESCM approach provides elastic boundary conditions for the atomistic domain by transferring the applied far field mechanical load through the continuum domain into the atomistic system.

The ESCM method is based on the concept that the continuum representation of a material, in terms of stress-strain fields, is a statistical representation of its atomic structure. Following this idea, the connection between the atomistic and the continuum representations at the MD/FE interface is performed using a statistical mechanics approach. The method uses statistical averaging over both time and volume of atomistic subdomains at the MD/FE interface to provide nodal displacement boundary conditions to the continuum FE domain. The FEM generates interface reaction forces that are uniformly distributed over the interface atoms in the form of constant traction boundary conditions^{10,11} to the MD domain. Thus, this approach is based on solving the special boundary value problem (BVP) at the MD/FE interface for a coupled MD-FEM system and may be described as a local-nonlocal BVP because it relates *local* continuum nodal quantities with statistical averages of *nonlocal* atomistic quantities over selected atomic volumes. For this study, one finite element at the interface encompasses a region of several hundred atoms, the positions of which have been averaged over a 1 ps time interval. At this scale, the discreteness of the atomic structure is sufficiently homogenized so that the FEM domain responds to the atomistic domain as an extension of the continuum. The constant traction boundary conditions of the MD domain ensure that the elastic field from the FEM domain is correctly transferred to the atomistic region. An iterative procedure using the MD statistical displacements establishes a balance between the FEM-computed forces and the MD-computed forces at the interface. This force balance ensures stress continuity at the interface.

The model geometry used to study transgranular crack propagation in an aluminum single crystal is shown in Fig. 1. A circular MD domain with a diameter $d_{\text{MD}} = 40$ nm was embedded in a square FEM mesh with side dimension $d_{\text{FE}} = 20d_{\text{MD}} = 0.8$ μm . In this model, the system represents a single crystal with a pre-inserted edge crack propagating along the x -direction. The crack plane normal is along the y -direction, and the crack front is along the z -direction. The crack from the continuum region is initially extended into the MD domain equal to $1/3 d_{\text{MD}}$ (see the enlarged central zone in the inset in Fig. 1). The atomically sharp crack tip in the MD domain is formed by screening the atomic forces between the atoms on both sides of the crack plane starting from the MD/FEM interface along a distance of $1/3 d_{\text{MD}}$ inside the MD domain.

The crack propagation direction, x , is fixed along the $[11\bar{1}]$ axis, so that the crack plane is perpendicular to the $(11\bar{1})$ slip plane. The crack front lies in the intersection of the $(11\bar{1})$ slip plane and the crack plane (Fig. 2). The orientation of the crack front line is chosen as the z -direction in the model. Under these circumstances, the only variable parameter for the crystallographic orientation of the crack is the twist angle, φ , formed between the crack plane normal (the y -direction in Fig. 2) and the $[112]$ twin axis, lying in the $(11\bar{1})$ slip plane. The reason behind this crystallographic setup is based on the Peierls criterion for deformation twinning suggested by Tadmor and Haim³. According to this criterion, the tilt angle, θ , between the slip plane and the crack plane does not affect the tendency of the crack tip to nucleate a twin or a full dislocation under mode I loading. This tendency depends only on the twist angle, φ . In this way, setting $\theta = 90^\circ$ is a convenient choice, because it permits the φ angle to vary while



keeping the crack front parallel to the most active $(11\bar{1})$ slip plane. Because of the symmetry of the f.c.c. lattice, one can only examine variations of φ between 0° and 30° . Altogether six values of φ have been considered here: $\varphi = 0^\circ, 13.90^\circ, 16.10^\circ, 19.11^\circ, 21.05^\circ$, and 30° that satisfy the crystallographics of the system. The corresponding crystallographic orientations of the crystal lattice are presented in Table 1. These orientations were chosen in order to examine values for φ around 15° , as will be discussed in Section III.

Figure 2: Crystallographic orientation of the crack with respect to the $(11\bar{1})$ slip plane in the f.c.c. lattice.

Periodic boundary conditions were applied in the z -direction of the MD system to emulate bulk atomic state. To achieve a correct calculation of the interatomic potential energy and force, the thickness h in the z -direction of the MD domain has to include a whole number of periods of

the crystal lattice in this direction. In addition, to ensure that at least 10 atomic planes are present in the z -direction (for consistency with the previous simulations by this group⁴), a condition $h > 2$ nm was imposed. The choices of h at 0 K for each value of φ are given in Table 1. The condition that the thickness in the z -direction is the same everywhere in the MD domain corresponds to a plane strain condition in the continuum domain.

φ [deg]	x	y	z	h [nm]
0	$[1 \ 1 \ \bar{1}]$	$[1 \ 1 \ 2]$	$[1 \ \bar{1} \ 0]$	2.864
13.90	$[1 \ 1 \ \bar{1}]$	$[2 \ 5 \ 7]$	$[4 \ \bar{3} \ 1]$	2.065
16.10	$[1 \ 1 \ \bar{1}]$	$[1 \ 3 \ 4]$	$[7 \ \bar{5} \ 2]$	3.577
19.11	$[1 \ 1 \ \bar{1}]$	$[1 \ 4 \ 5]$	$[3 \ \bar{2} \ 1]$	3.031
21.05	$[1 \ 1 \ \bar{1}]$	$[1 \ 5 \ 6]$	$[11 \ \bar{7} \ 4]$	2.762
30	$[1 \ 1 \ \bar{1}]$	$[0 \ 1 \ 1]$	$[2 \ \bar{1} \ 1]$	2.976

Table 1: Crystallographic orientations of the crystal lattice and thickness, h , of the MD system for the applied set of φ - angles.

The system has been loaded in uniaxial tension along the y -axis, through applying uniform displacement boundary conditions on the outer boundaries of the FEM square domain. The resulting stress intensity at the crack tip follows the continuum definition for K_I for the presented geometry¹². The loading started from zero strain, $\epsilon = 0$, and was incremented by 0.1% every 20 ps of simulation time, equivalent to a strain rate of 5×10^7 s⁻¹. The applied strain increments of 0.1% resulted in increments of the stress intensity at the initial crack tip of $K_I = 0.049$ MPa-m^{1/2}. The strain rate was sustained until a nano-twin or a full dislocation was emitted from the crack tip. The average stress along the periodic z -direction in the MD domain was maintained at zero by applying the Parrinello-Rahman constant stress technique¹³. The MD system was simulated at constant temperature (300K) using the Nose-Hoover thermostat¹⁴.

To analyze the processes taking place in the atomistic domain, the common-neighbor-analysis (CNA) technique was applied¹⁵. CNA identifies the local crystallographic state of an

atom based on the relative positions of its neighbors. For this study, two specific crystallographic states were of interest: the f.c.c. state – the ground state – and the h.c.p. state, which indicates a twin boundary (a single plane of h.c.p. atoms) or a stacking fault (a double plane of h.c.p. atoms). Atoms that were not identified as being in either of these two states were considered as disordered atoms. In a single crystal, the disordered atoms indicate a dislocation core or a vacancy. In addition, atoms that have lost more than 1/3 of its neighbors in the vicinity of their interaction range were considered as free surface atoms. In this model surface atoms indicate the crack surface. In the simulation snapshots presented in the paper (e.g., Figs. 3, 6 and 7, discussed in Section III), atoms in these various crystallographic states were color-coded to aid in visualization. All atoms in an f.c.c. state were colored in grey, and f.c.c. atoms that interface with the FEM nodes^{6,7} were colored in dark-gray. Atoms in h.c.p. state were colored in red, disordered atoms were colored in blue and surface atoms were colored in brown. For example, in Section III, the consecutive emission of the three partial dislocations, formations d1, d2, and d3 seen as blue dots in Fig. 3(a), produce a nano-twin indicated by parallel red lines that begin at the crack tip.

III. Results and Analysis

III.1. Twin-dislocation transition with orientation

The first set of simulations was performed to study the initiation process of a twin or a full dislocation emission from the crack tip during crack propagation under mode I loading. As explained in Section II, the crack was gradually loaded by increasing the applied tensile strain in the FEM domain and monitoring the processes at the crack tip in the MD domain. The initial twin or dislocation nucleation for all six simulated crystallographic orientations is given in Fig. 3. The nucleation process was first observed when the stress intensity reached $K_I = 0.34 \text{ MPa-m}^{1/2}$. However, because of the incremental increase of K_I in steps of 0.049 (see Sec. II), the critical stress intensity K_{IC} , at which the first dislocation $d1$ in Fig. 3 is nucleated, was estimated to be between 0.29 and 0.34 $\text{MPa-m}^{1/2}$.

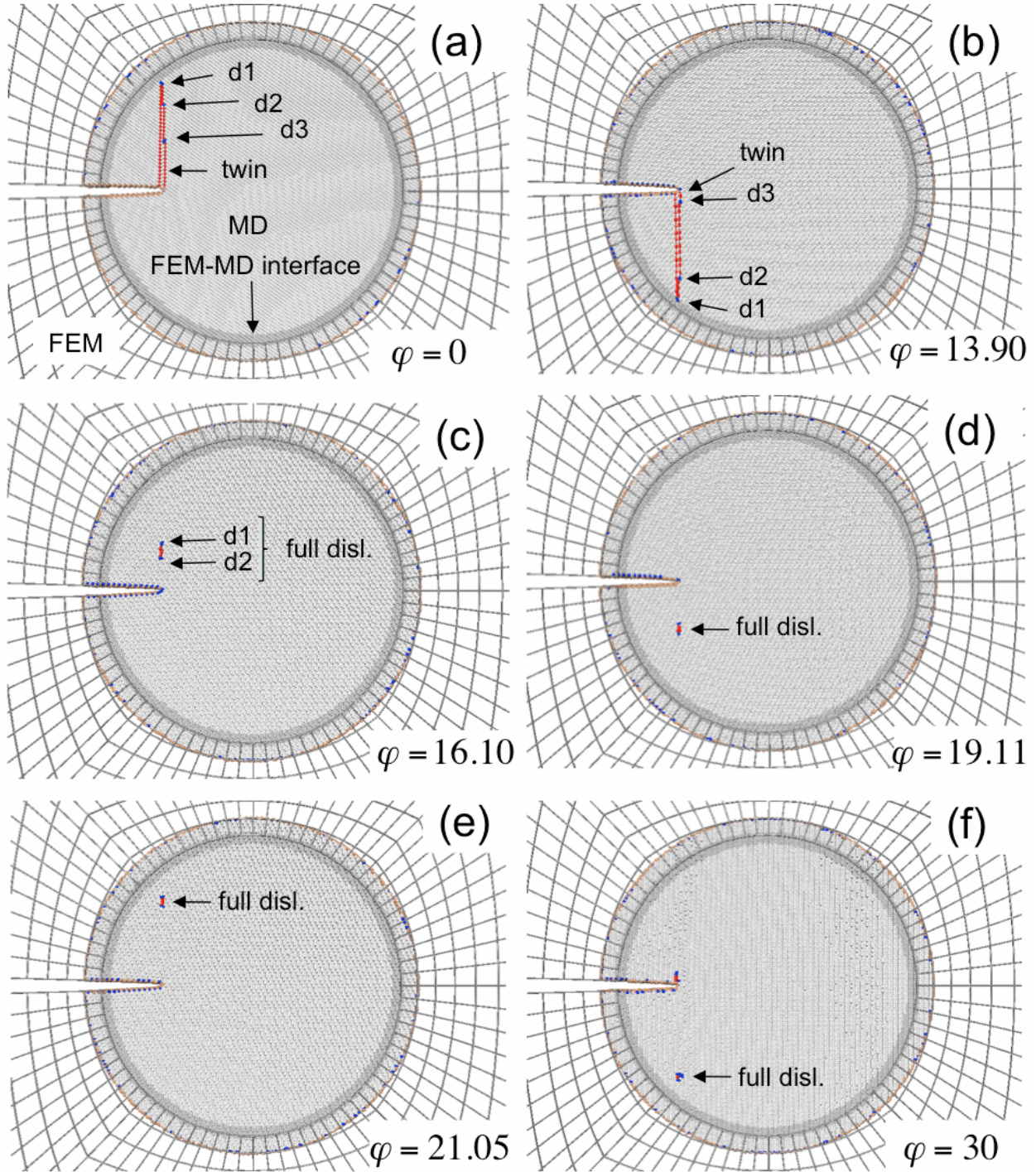


Figure 3: Simulation snapshots of the initiation of plastic processes at the crack tip for the set of orientations given in Table 1.

To distinguish between the occurrences of twinning or full dislocation emission, at least two of the dislocations nucleated from the crack tip (d1 and d2 in Fig. 3) need to be examined. If the second dislocation leaves an extrinsic stacking fault¹⁵ behind, indicated by two parallel lines of

h.c.p. atoms separated by one line of f.c.c. atoms¹⁶ (Fig. 3a and Fig. 3b), then a nano-twin nucleation has taken place^{15,16}. Further emissions of dislocations would most likely broaden the nano-twin¹⁵ as the third dislocation has done in Fig. 3(a) and Fig. 3(b). If the second dislocation terminates the stacking fault left behind the first dislocation (Figs. 3c-f) then a full dislocation (consisted of two partial dislocations, $d1 + d2$ in Fig. 3c) emission has taken place.

The snapshots in Fig. 3 indicate a transition from twin nucleation to full dislocation nucleation during changes in the angle φ from 0° to 30° . The Thompson Triangle¹⁷ shown in Fig. 4 is now used to illustrate the transition from twinning to full dislocation nucleation in the active $(1\bar{1}\bar{1})$ slip plane. At $\varphi = 0^\circ$ (Fig. 4a) the direction of the tensile load, the y -direction, is parallel to the twinning direction $[112]$. In this case, both nucleated partial dislocations, $d1$ and $d2$, are of the same type with Burgers vectors in the $[112]$ direction. This is the situation when a twin is formed. At $\varphi = 13.90^\circ$ (Fig. 4b), the Thompson triangle is slightly rotated in a clockwise direction, so that the y -direction of the tensile load is slightly inclined to the twin direction $[112]$, but the inclination angle φ is too small to affect the dislocation nucleation process. The dislocation nucleation process is similar to that in Fig. 4(a), and twinning still takes place. However, further increase of the angle φ does change the deformation mode from twinning to full dislocation emission. At $\varphi = 16.10^\circ$ (Fig. 4c), the second dislocation $d2$ is nucleated in the $[1\bar{2}\bar{1}]$ direction. Both partial dislocations, $d1$ and $d2$, combined to form a full dislocation $d3$ with a resultant Burgers vector along the $[011]$ direction. The same situation occurs for the remainder of the φ angles as indicated in Figs. 4(d-f).

A simplified but illustrative explanation of the change in the deformation mode from twinning to full dislocation emission can be given. Deformation twinning produces displacements in the crystal lattice along the $<112>$ family of directions through the consecutive emission of parallel Shockley partial dislocations¹⁵ such as $d1$ and $d2$ in Fig. 4(a) and Fig. 4(b). Full dislocation emission produces displacement along the $<110>$ family of directions by the emission of two Shockley partial dislocations in non-parallel $<112>$ directions with a combined Burgers vector along one of the $<110>$ directions. Schematically, this is shown in Figs. 4(c-f) where the combined dislocation $d3$ is formed as a sum of the two non-parallel partial dislocations, $d1$ and $d2$. When $\varphi < 15^\circ$, the tensile y -direction is closer to the $[112]$ direction (Fig. 4a and Fig. 4b) and the displacement takes place in the $[112]$ direction, which results in twinning. When $\varphi > 15^\circ$, the

tensile y -direction is closer to the $[011]$ direction (Figs. 4c-f), and it is more favorable for the displacement to take place in the $[011]$ direction. In order for this to happen, the second partial dislocation $d2$ is nucleated in the $[\bar{1}\bar{2}\bar{1}]$ direction so that the total Burgers vector of $d1$ and $d2$ produces a displacement along the $[011]$ direction.

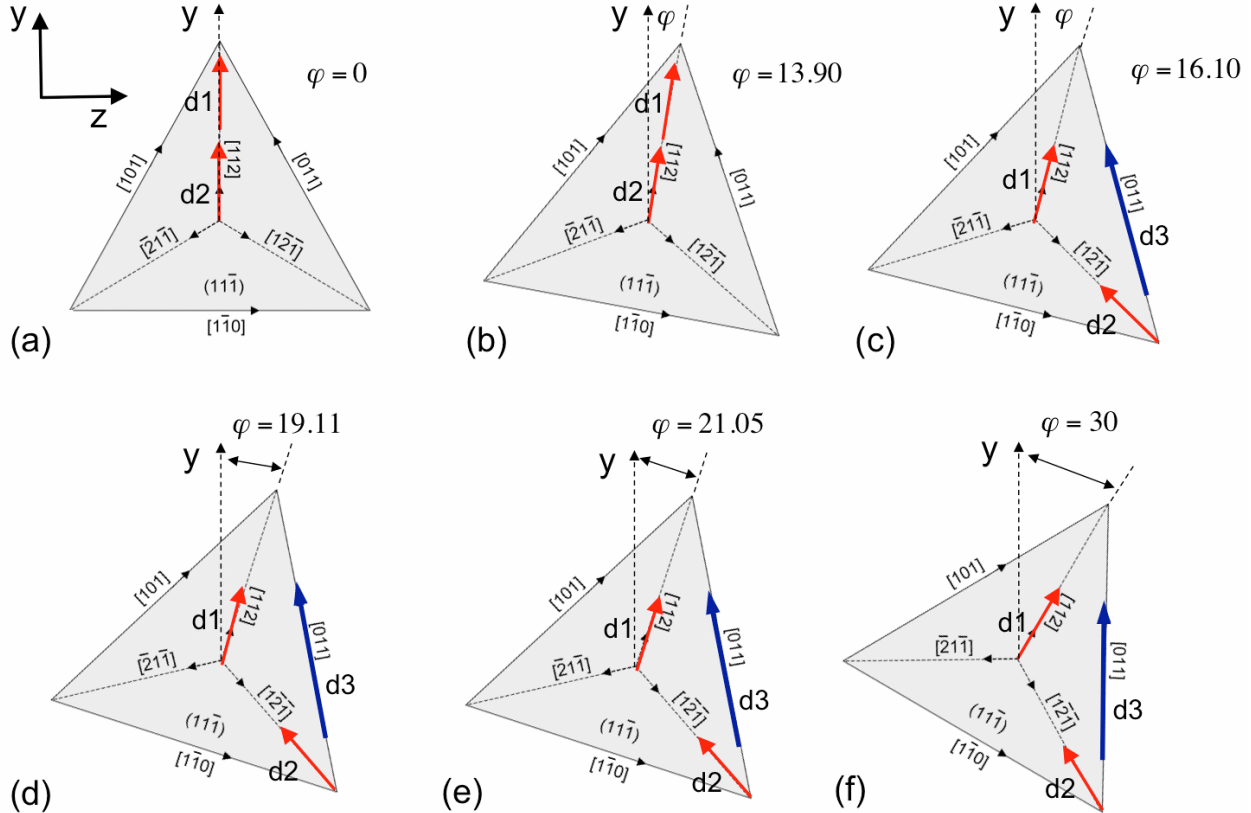


Figure 4: Crystallographic orientations of the $(11\bar{1})$ slip system at the crack tip in Thompson schematics for the set of orientations given in Table 1.

A more rigorous analysis of the process is given by Tadmor and Hai³. They calculate the critical stress intensities, K_{IC}^{twin} and K_{IC}^{disl} , required to nucleate a pair of parallel (for twinning) or non-parallel (for full dislocation emission) Shockley partials under a given direction of loading and crystal orientation. If $K_{IC}^{twin} < K_{IC}^{disl}$ then twinning is the more energetically favorable process and is more likely to occur. If $K_{IC}^{disl} < K_{IC}^{twin}$ then full dislocation emission is the energetically

more favorable result. Based on this consideration, Tadmor and Hai³ proposed a criterion for twinning against full dislocation emission as the ratio between K_{IC}^{disl} and K_{IC}^{twin}

$$T(\varphi) = \frac{K_{IC}^{disl}}{K_{IC}^{twin}} \quad \begin{cases} T > 1 & \text{twinning} \\ T < 1 & \text{dislocation} \end{cases} \quad . \quad (1)$$

For the case of pure mode I loading, the calculations show³ that, while K_{IC}^{disl} and K_{IC}^{twin} separately depend on the tilt angle θ (Fig. 2), their ratio $T(\varphi)$ does not. In this way, the results for $\theta = 90^\circ$, presented in this work, are representative for all tilt angles scenarios. Using the methodology by Tadmor and Hai³ to calculate $K_{IC}^{disl}(\varphi)$ and $K_{IC}^{twin}(\varphi)$ for the energetically most favorable pair of partial dislocations, the dependence of their ratio $T(\varphi)$ on φ for aluminum is given in Fig. 5. The material parameters that enter into the calculation³ are the stable and unstable stacking fault energies, written as γ_{sf} and γ_{us} , respectively, as defined by Rice¹⁸, and the unstable twinning energy, γ_{ut} , as defined by Tadmor and Hai³. These energies for the curve, presented in Fig. 5, were derived from the interatomic potential⁹ at $T = 0$ K. The specific values are given as⁹: $\gamma_{sf} = 0.146 \text{ J/m}^2$, $\gamma_{us} = 0.168 \text{ J/m}^2$, and⁴ $\gamma_{ut} = 0.21 \text{ J/m}^2$. It is expected that their values at $T = 300$ K are slightly lower, and the curve on Fig. 5 may not be quantitatively representative for $T = 300$ K, but it is given here for qualitative analysis.

From a qualitative point of view, Fig. 5 shows a maximum value of $T(\varphi)$ at $\varphi = 0^\circ$ and a minimum at $\varphi = 30^\circ$. Thus, twinning is expected at $\varphi = 0^\circ$ and full dislocation emission is expected at $\varphi = 30^\circ$, which is in agreement with the simulation results in Fig. 4(a) and Fig. 4(f). It should be noted however, that the range where $T(\varphi) > 1$ in Fig. 5 is very narrow (about $\pm 1^\circ$), while the MD simulations show a predominant twinning in a broader range up to $\varphi = 13.9^\circ$ (Fig. 4b). One possible explanation for this quantitative disagreement could be that the analytical curve in Fig. 5 is given for $T = 0$ K, while the simulations were performed for $T = 300$ K. A more likely explanation is that the analytical curve is based on a minimum energy consideration and represents a static case, while the simulations are dynamic and were performed at a very high strain rate of $5 \times 10^7 \text{ s}^{-1}$. The mechanisms by which the strain rate may affect the twin-dislocation transition, as found in the atomistic simulations, are discussed in the next subsection.

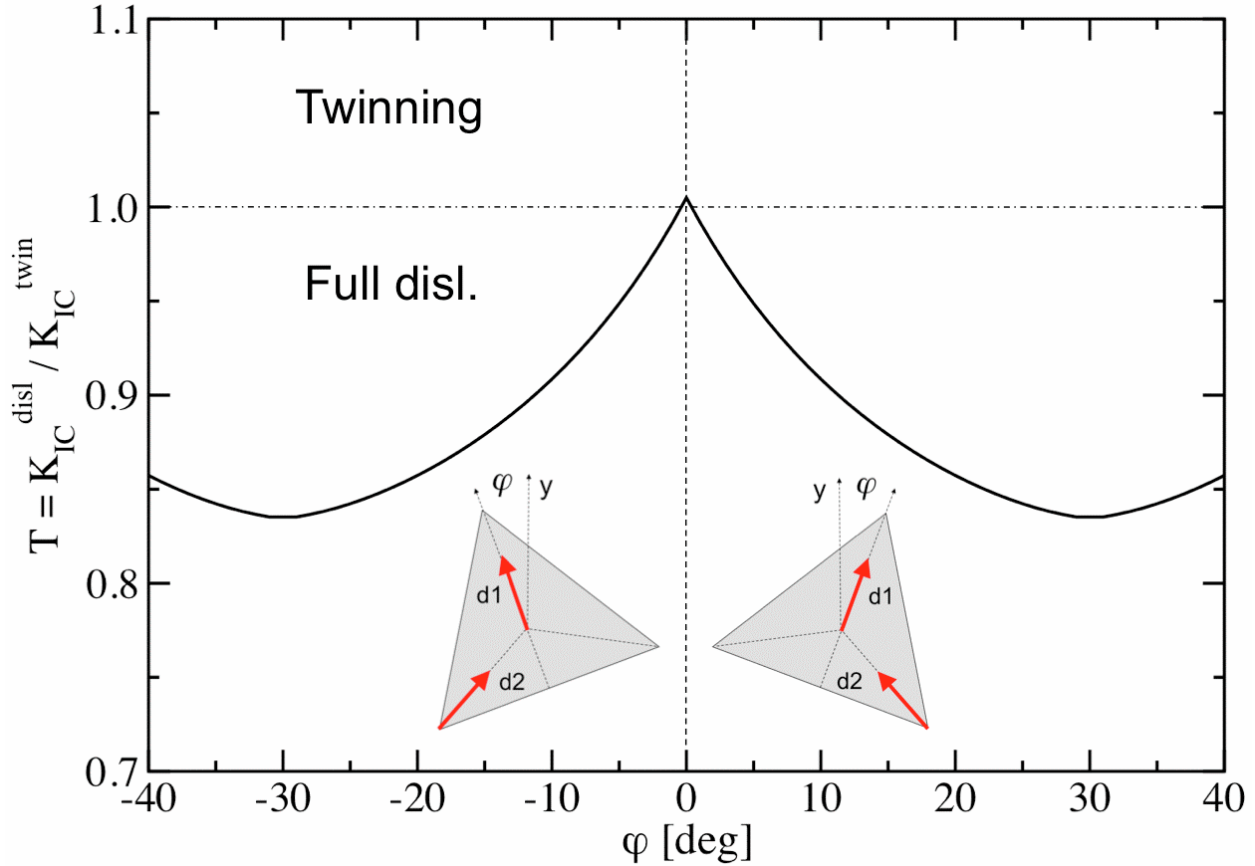


Figure 5: Orientation dependence of the Tadmor-Hai criterion for deformation twinning at a crack tip in aluminum.

III.2. Twin-dislocation transition with stress intensity

The effect of the high strain rate, inherently present in molecular-dynamics simulations, on the crack tip twinning in aluminum has recently been discussed by Warner et al.⁵ The main consideration in that work⁵, based on transition state theory¹⁹, was that to observe a dislocation nucleation from the crack tip in an MD simulation time frame (a few nanoseconds), the dislocation nucleation rate must be on the order of 10^9 - 10^{10} events per second. To achieve this high nucleation rate, much larger stress intensities have to be applied as compared to experimental conditions, where a nucleation rate of 10^0 - 10^1 is usually enough to observe dislocation nucleations in the time frame of seconds. The role of the stress intensity on the nucleation rate is accounted for in the Rice and Beltz model²⁰ of dislocation nucleation at a crack tip. The analysis⁵ has shown that a transition stress intensity for twinning K_{IT} exists, at which the deformation mode changes from full dislocation emission to deformation twinning. For the case $\varphi = 0^\circ$, considered as a typical twinning case⁵, K_{IT} was found to be substantially lower than

values of K_I that are commonly observed in MD simulations of crack propagation. For a full dislocation emission to take place, the condition $K_I < K_{IT}$ has to be fulfilled. However, according to transition state theory^{5,19}, the dislocation nucleation rate at $K_I < K_{IT}$ is so low that to record a dislocation emission event the observation time in the MD simulation has to be increased by more than four orders of magnitude to the level of 10^{-5} s (equivalent to a strain rate of 10^{-3} s⁻¹ for 1% deformation). To achieve this slowdown, an advanced coupled multiscale-accelerated dynamics technique, which involved scaling on both, space and time scales, was applied⁵.

Warner et al. calculations⁵ for the transition from deformation twinning to full dislocation nucleation were found to agree qualitatively with the theoretical predictions, but substantial quantitative differences were also apparent, indicating that further study is needed to fully understand the process. The complexity of the applied multiscale-accelerated dynamics technique by Warner et al.⁵ made its use more difficult in a more systematic study of the problem. A different approach is presented in the present paper, which allows the twin-dislocation transition to be reproduced and studied at the MD-accessible strain rate of 5×10^7 s⁻¹. This permits the more computationally affordable conventional MD technique to be used and avoids some possible artifacts of applying an accelerated-dynamics technique.

The new approach is based on the observed MD twin-dislocation transition with the change of crystal orientation as described in Sec. III.1. The observed transition from twinning to full dislocation emission shown in Fig. 4 can be interpreted as a result of increasing the transition stress intensity, K_{IT} , as φ varies from 0 to 30°. Thus, at some intermediate angle, φ , between 13.9° and 16.1°, K_{IT} becomes higher than the applied stress intensity K_I , and twinning is replaced by full dislocation emission. If this is indeed the case, then increasing the applied stress intensity above K_{IT} would reinitiate the twinning mechanism, whereas full dislocation emissions were initially observed at lower stress intensities. This scenario is easier to test by MD simulations than the case studied by Warner et al.⁵, because in an MD simulation, an increase of K_I is much easier to achieve than a decrease, as it avoids the use of accelerated dynamics techniques. The drawback is that increasing the stress intensity may induce additional deformation modes, such as the activation of a secondary slip system, as seen in Fig. 6, which will be discussed next.

To examine the dependence of the twin-dislocation transition on increasing stress intensity, the first two values of φ , equal to $\varphi = 16.10^\circ$ and $\varphi = 19.11^\circ$, were selected because they emitted full dislocations. The systems were subject to four levels of uniaxial tensile strain of $\epsilon_{yy} = 0.7\%$,

0.8%, 0.9%, and 1.0% corresponding to $K_I = 0.34, 0.39, 0.44$, and $0.49 \text{ MPa}\cdot\text{m}^{1/2}$, respectively. The results for $\varphi = 16.10^\circ$ are shown in Fig. 6. At $K_I = 0.34 \text{ MPa}\cdot\text{m}^{1/2}$ (Fig. 6a), the crack emitted a full dislocation and at $K_I = 0.39 \text{ MPa}\cdot\text{m}^{1/2}$, a twin was nucleated (Fig. 6b). Twin nucleation continued to be systematically observed at higher loads of $K_I = 0.44$, and $0.49 \text{ MPa}\cdot\text{m}^{1/2}$ (Figs. 6c and 6d). From these results, it follows that the transition stress intensity at $\varphi = 16.10^\circ$ is approximately $K_{IT} = 0.39 \text{ MPa}\cdot\text{m}^{1/2}$. Similar behavior is found for $\varphi = 19.11^\circ$, as shown in Fig. 7, but twinning starts at a higher load of $K_I = K_{IT} = 0.49 \text{ MPa}\cdot\text{m}^{1/2}$. Thus, an increase in φ results in an increase in K_{IT} by the same mechanisms that were observed in Fig. 6. The high stress at which twinning starts, induces the emission of partial dislocations on a secondary slip plane as seen in Figs. 6(c,d) and Figs. 7(c,d).

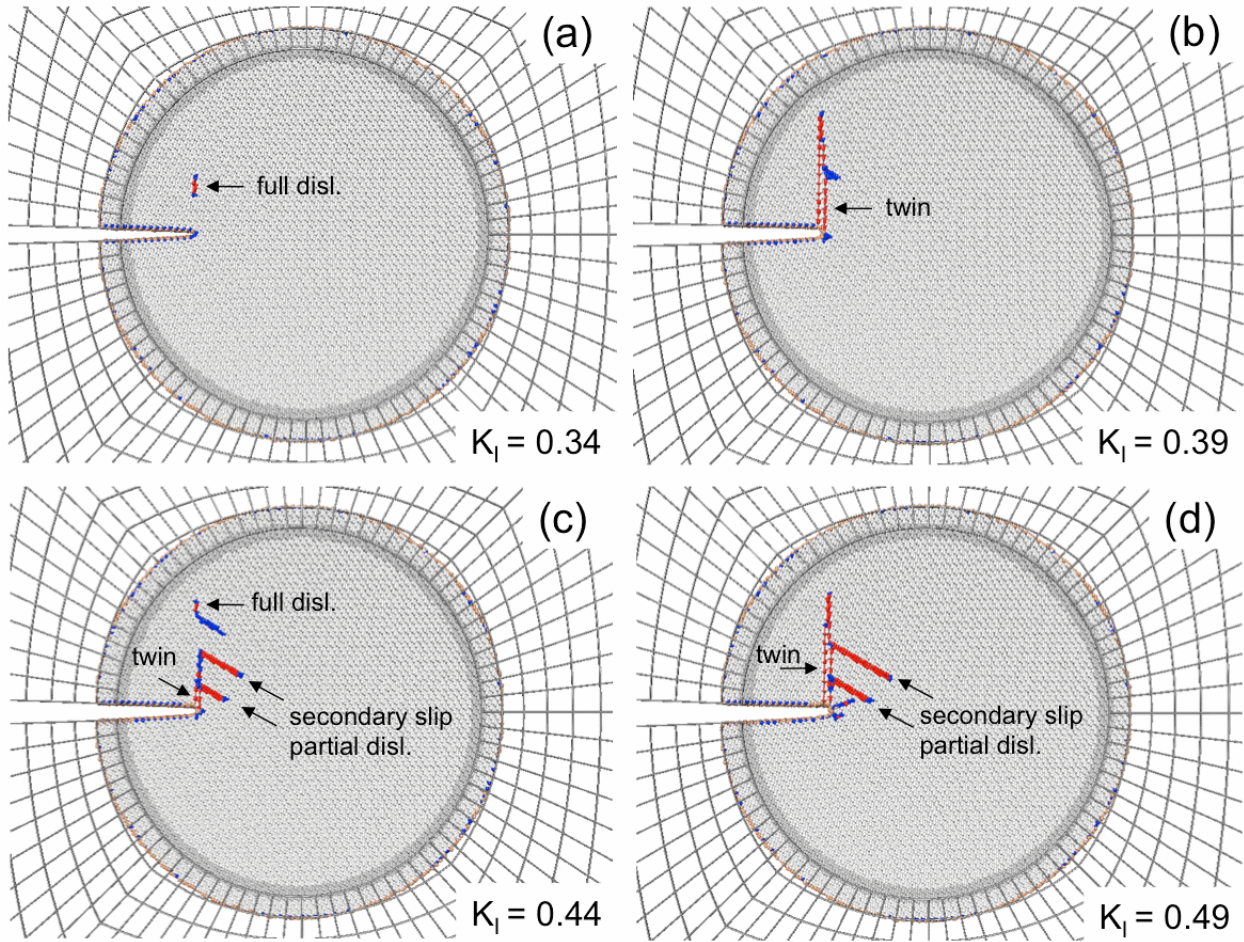


Figure 6: Simulation snapshots of the initiation of plastic processes at the crack tip for $\varphi = 16.10^\circ$ at different stress intensities K_I , as indicated in the figure.

The presented results confirm the conclusion of Warner et al.⁵ that a transition stress intensity K_{IT} exists, below which the crack emits full dislocations, and above which deformation twinning takes place. The results also show that K_{IT} is a function of the twist angle φ . At $\varphi = 0$, K_{IT} is too low for a dislocation nucleation event to take place at typical MD time scales and full dislocation emission cannot be seen in a conventional MD simulation at this orientation. At orientations for which K_{IT} is above the simulated K_I , full dislocation emission becomes the dominant crack propagation mode. When K_I is increased above K_{IT} , deformation twinning is again observed.

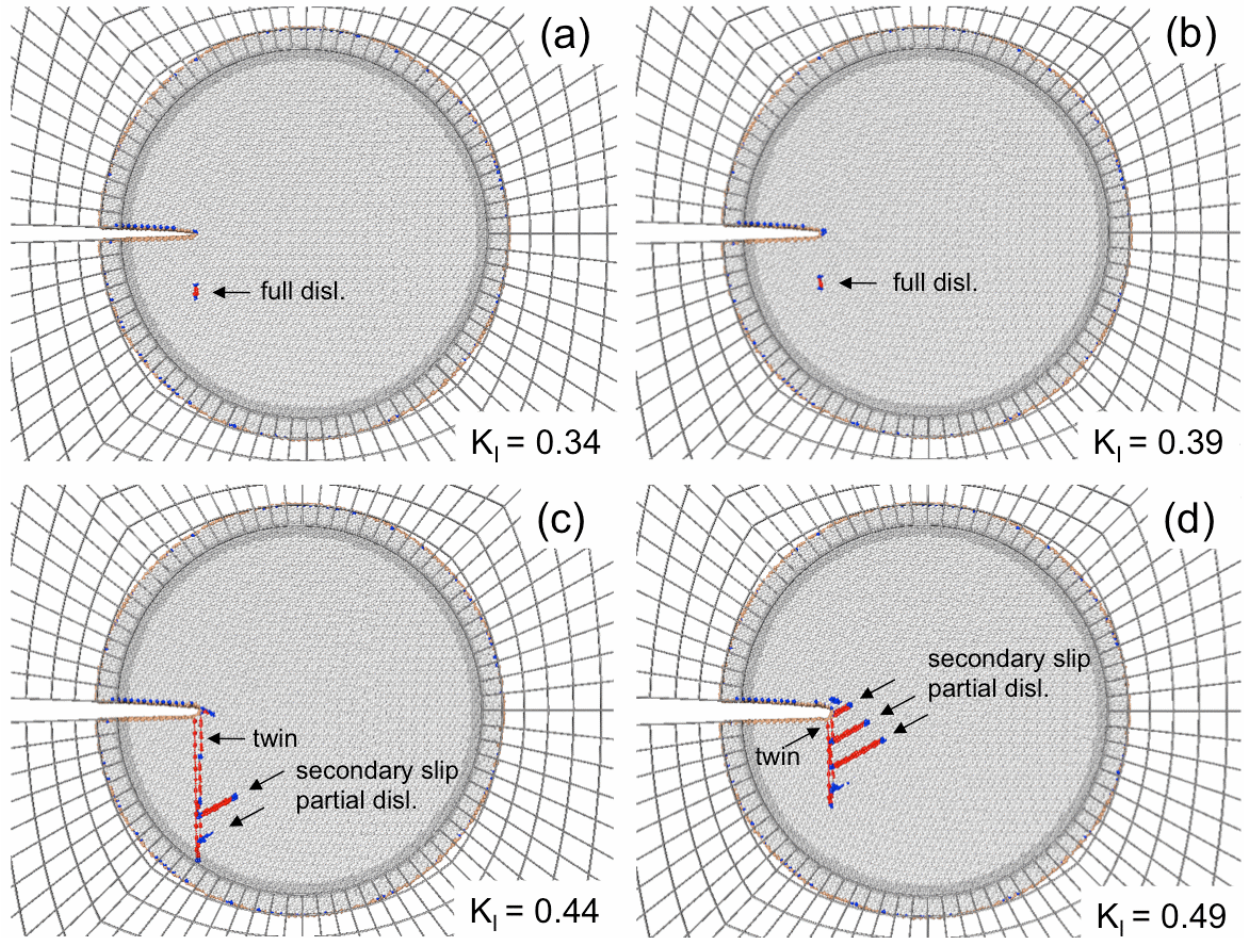


Figure 7: Simulation snapshots of the initiation of plastic processes at the crack tip for $\varphi = 19.11^\circ$ at different stress intensities K_I , as indicated in the figure.

IV. Summary

The simulation method for this study is based on the embedded statistical coupling method (ESCM). The ESCM is a MD-FEM coupling method, which uses statistical quantities such as statistically averaged atomic displacements to connect the atomistic MD domain with the continuum FE domain. As a consequence, the ESCM technique makes possible relatively large atomistic domains (10^5 to 10^7 atoms) to be embedded in a continuum domain of micrometer dimensions. This capability is essential for the present study because it minimizes the finite size effects by allowing edge cracks of $0.45\text{ }\mu\text{m}$ size to be modeled while preserving the atomic representation of the material at the crack tip. The ESCM method so far has been successfully applied in the case of intergranular fracture, where the crack propagation direction was predefined by the existing grain boundary. The presented study is the first application of the ESCM approach for the case of transgranular fracture.

Dislocation processes at a crack tip in a single crystal of pure aluminum were studied. Two types of processes were found to take place: deformation twinning and emission of full dislocations (i.e. dislocation slip at the crack tip). Studying the transition between these two processes reveals the existence of a transition stress intensity, K_{IT} , below which the crack emits full dislocations and above which deformation twinning becomes dominant. The transition stress intensity depends on the crystallographic orientation of the crack front in mode I loading, through the twist angle φ between the tensile direction and the twinning [112] crystallographic axis. A minimum value of K_{IT} is reached at $\varphi = 0^\circ$ where twinning becomes the dominant crack propagation mode in MD simulations due to their inherently very high strain rates of 10^7 s^{-1} or higher. A maximum value of K_{IT} at $\varphi = 30^\circ$ defines the region of full dislocation emission at typical MD time scales. To be consistent with experimental observations, where deformation twinning at the crack tip in aluminum is rarely observed, this study suggests that crystallographic orientations close to $\varphi = 30^\circ$ should be used for atomistic characterization of crack tip plastic processes in aluminum. Orientations close to $\varphi = 0^\circ$ should be avoided as they produce the artifact of deformation twinning, that can substantially alter the predicted fracture parameters, such as the peak stress of debonding and energy of decohesion.

V. Acknowledgments

V. Yamakov is sponsored through cooperative agreement NCC-1-02043 with the National Institute of Aerospace.

VI. References

¹Farkas, D., Duranduru, M., Curtin, W. A., Ribbens, C, "Multiple-Dislocation Emission from the Crack Tip in the Ductile Fracture of Al," *Phil. Mag., A* **81**, 2001, pp. 1241-1255.

²Hai, S., Tadmor, E. B., "Deformation Twinning at Aluminum Crack Tips," *Acta Mater.*, **51**, 2003, pp. 117-131.

³Tadmor, E. B., Hai, S., "A Peierls Criterion for the Onset of Deformation Twinning at a Crack Tip," *J. Mech. Phys. Solids*, **51**, 2003, pp. 765-793.

⁴Yamakov, V., Saether, E., Phillips, D. R., Glaessgen, E. H., "Molecular-Dynamics Simulation-Based Cohesive Zone Representation of Intergranular Fracture Processes in Aluminum," *J. Mech. Phys. Solids*, **54**, 2006, pp. 1899-1928.

⁵Warner, D. H., Curtin, W. A., Qu, S., "Rate dependence of Crack-Tip Processes Predicts Twinning Trends in f.c.c. Metals," *Nature Mater.*, **6**, 2007, pp. 876-880.

⁶Saether, E., Yamakov, V., Glaessgen, E.H., "A Statistical Approach for the Concurrent Coupling of Molecular Dynamics and Finite Element Methods," *Proceedings of the 48th AIAA/ASME/ASCE/AHS/ASC Structures, Structural Dynamics, and Materials Conference*, AIAA-2007-2169-CP, AIAA, Honolulu, HI, April 23-26, 2007.

⁷Saether, E., Yamakov, V., Glaessgen, E.H., "An Embedded Statistical Method for Coupling Molecular Dynamics and Finite Element Analyses," *Int. J. Num. Methods Eng.*, 2009, (in press).

⁸Yamakov, V., Saether, E., Glaessgen, E. H., "Multiscale Modeling of Intergranular Fracture in Aluminum: Constitutive Relation for Interface Debonding," *J. Mat. Sci.*, **43**, 2008, pp. 7488-7494.

⁹Mishin, Y., Farkas, D., Mehl, M. J., Papaconstantopoulos, D. A., "Interatomic potentials for monoatomic metals from experimental data and ab initio calculations," *Phys. Rev. B*, **59**, 1999, pp. 3393-3407.

¹⁰Cheung, K. S., Yip, S., "A Molecular-Dynamics Simulation of Crack-Tip Extension: The Brittle-To-Ductile Transition," *Modelling Simul. Mater. Sci. Eng.*, **2**, 1994, pp. 865-892.

¹¹Cleri, F., "Representation of mechanical loads in molecular dynamics simulations," *Phys. Rev. B*, **65**, 2001, pp. 014107-1-10.

¹²Murakami, Y. (Editor-in-Chief), "Stress Intensity Factors Handbook," vol. 1, *Pergamon Press, New York*, 1987, p. 99.

¹³Parrinello, M., Rahman, A., "Polymorphic Transitions in Single Crystals; A New Molecular Dynamics Method," *J. Appl. Phys.*, **52**, 1981, pp. 7182-7190.

¹⁴Nose, S., "A Unified Formulation of the Constant Temperature Molecular Dynamics Method," *J. Chem. Phys.*, **81**, 1984, pp. 511-519.

¹⁵Weertman, J., Weertman, J. R., "Elementary dislocation theory," Oxford University Press, New York, 1992.

¹⁶Schiotz, J., Vegge, T., Di Tolla, F. D., Jacobsen, K. W., "Atomic-scale simulations of the mechanical deformation of nanocrystalline metals," *Phys. Rev. B*, **60**, 1999, pp. 11971-11983.

¹⁷Thompson, N. *Proc. Phys. Soc.*, **66 B**, 1953, pp. 481.

¹⁸Rice, J. R., "Dislocation Nucleation from a Crack Tip: An Analysis Based on the Peierls Concept," *J. Mech. Phys. Solids*, **40**, 1992, pp. 239-271.

¹⁹Eyring, H., "The Activated Complex in Chemical Reactions," *J. Chem. Phys.*, **3** 1935, pp. 107-115.

²⁰Rice, J. R., Beltz, G. E., "The Activation Energy for Dislocation Nucleation at a Crack," *J. Mech. Phys. Solids*, **42**, 1994, pp. 333-360.